AEDC-TR-76-140

Cy. 1

[redacted]

CORRECTIONS TO SINGLE-SHIELDED TOTAL TEMPERATURE PROBES IN SUBSONIC, SUPERSONIC, AND HYPERSONIC FLOW

VON KÁRMÁN GAS DYNAMICS FACILITY
ARNOLD ENGINEERING DEVELOPMENT CENTER
AIR FORCE SYSTEMS COMMAND
ARNOLD AIR FORCE STATION, TENNESSEE 37389

November 1976

Final Report for Period October 1975 - August 1976

[redacted]

Approved for public release; distribution unlimited.

Prepared for

DIRECTORATE OF TEST (XO)
ARNOLD ENGINEERING DEVELOPMENT CENTER
ARNOLD AIR FORCE STATION, TENNESSEE 37389

NOTICES

When U. S. Government drawings specifications, or other data are used for any purpose other than a definitely related Government procurement operation, the Government thereby incurs no responsibility nor any obligation whatsoever, and the fact that the Government may have formulated, furnished, or in any way supplied the said drawings, specifications, or other data, is not to be regarded by implication or otherwise, or in any manner licensing the holder or any other person or corporation, or conveying any rights or permission to manufacture, use, or sell any patented invention that may in any way be related thereto.

Qualified users may obtain copies of this report from the Defense Documentation Center.

References to named commercial products in this report are not to be considered in any sense as an endorsement of the product by the United States Air Force or the Government.

This report has been reviewed by the Information Office (OI) and is releasable to the National Technical Information Service (NTIS). At NTIS, it will be available to the general public, including foreign nations.

APPROVAL STATEMENT

This technical report has been reviewed and is approved for publication.

FOR THE COMMANDER

Keith L. Kushman

KEITH L. KUSHMAN
Captain, USAF
Analysis and Evaluation Division
Directorate of Test

Alan L. Devereaux

ALAN L. DEVEREAUX
Colonel, USAF
Director of Test

REPORT DOCUMENTATION PAGE		READ INSTRUCTIONS BEFORE COMPLETING FORM
1. REPORT NUMBER AEDC-TR-76-140	2. GOVT ACCESSION NO.	3. RECIPIENT'S CATALOG NUMBER
4. TITLE (and Subtitle) CORRECTIONS TO SINGLE-SHIELDED TOTAL TEMPERATURE PROBES IN SUBSONIC, SUPERSONIC, AND HYPERSONIC FLOW		5. TYPE OF REPORT & PERIOD COVERED Final Report - October 1975 - August 1976 6. PERFORMING ORG. REPORT NUMBER
7. AUTHOR(s) M. O. Varner, ARO, Inc.		8. CONTRACT OR GRANT NUMBER(s)
9. PERFORMING ORGANIZATION NAME AND ADDRESS Arnold Engineering Development Center (XO) Air Force Systems Command Arnold Air Force Station, Tennessee 37389		10. PROGRAM ELEMENT, PROJECT, TASK AREA & WORK UNIT NUMBERS Program Element 65807F
11. CONTROLLING OFFICE NAME AND ADDRESS Arnold Engineering Development Center(DYFS) Arnold Air Force Station Tennessee 37389		12. REPORT DATE November 1976 13. NUMBER OF PAGES 34
14. MONITORING AGENCY NAME & ADDRESS(if different from Controlling Office)		15. SECURITY CLASS. (of this report) UNCLASSIFIED 15a. DECLASSIFICATION DOWNGRADING SCHEDULE N/A

16. DISTRIBUTION STATEMENT (of this Report)

Approved for public release; distribution unlimited.

17. DISTRIBUTION STATEMENT (of the abstract entered in Block 20, if different from Report)

18. SUPPLEMENTARY NOTES

Available in DDC

19. KEY WORDS (Continue on reverse side if necessary and identify by block number)

temperature measuring instruments
probes
corrections
wind tunnels

20. ABSTRACT (Continue on reverse side if necessary and identify by block number)

A new total temperature measurement correction is developed for the single-shielded type of probe. This method is based on a detailed analysis of the coupled heat transfer-viscous flow region existing within the probe. The correction is valid for all flow-field conditions and requires probe calibration data only in the free stream where flow properties are known. Total temperature measurements on the windward ray of a 4-deg sharp cone at Mach 10

DD FORM 1 JAN 73 1473 EDITION OF 1 NOV 65 IS OBSOLETE

20. ABSTRACT (Continued)

in AEDC Hypersonic Tunnel (C) are used in conjunction with corresponding theoretical predictions to substantiate the present analysis. The new approach appears to be a significant improvement over present methods.

AFSC
Arnold AFS Tenn

PREFACE

The work reported herein was conducted by the Arnold Engineering Development Center (AEDC), Air Force Systems Command (AFSC), under Program Element 65807F. The results were obtained by ARO, Inc. (a subsidiary of Sverdrup & Parcel and Associates, Inc.), contract operator of AEDC, Arnold Air Force Station, Tennessee. The research was done under ARO Project Nos. V43A-07A and V43A-16A. The author of this report was M. O. Varner, ARO, Inc. The manuscript (ARO Control No. ARO-VKF-TR-76-95) was submitted for publication on August 20, 1976.

The work of Mr. D. E. Boylan in obtaining the experimental data in Tunnel C and Dr. J. C. Adams in providing the Lubard hypersonic viscous shock layer (HVSL) theoretical results is acknowledged.

CONTENTS

ILLUSTRATIONS

TABLE

1.0 INTRODUCTION

The total temperature probe currently used in the von Kármán Gas Dynamics Facility (VKF) at AEDC is of the single-shielded type as developed by Bontrager (Ref. 1). He considered the cumulative effects of radiation loss to the walls, velocity, and conduction in defining the optimum probe configuration for a given flow environment. Probe calibration was accomplished by defining the relationship of actual-to-measured total temperature in the free stream at Mach 8 and 10 with the ratio of estimated entrance length of underdeveloped flow to a characteristic probe length. An experimental parametric analysis revealed an optimum probe entrance length-to-internal diameter ratio of two and probe entrance-to-vent area ratio of two or greater over the range of variables investigated.

Recent use of Bontrager's method for total temperature probe corrections has pointed out a shortcoming of his approach. As long as the calibration and corrections are made over approximately the same Mach number and probe Reynolds number range, the method appears to give consistent results. Use of an extrapolated calibration curve to correct total temperature measurements in an uncalibrated Mach number and/or probe Reynolds number range has led to inconsistent results when compared to theoretical predictions.

Others, for example, Winkler (Ref. 2) and Voisinet, Lee, and Meier (Ref. 3), have included a Mach number effect based on the total temperature recovery of cylinders in compressible flow. This approach as applied to a somewhat different probe design appears to give an improved correction to the total temperature measurements. Apart from the correction for Mach number effect, the inaccuracy still exists in extrapolating a calibration curve based on tunnel free-stream conditions to points outside of the calibration range in order to correct total temperature measurements (for instance, within boundary layers).

An examination of the methods to correct total temperature measurements proposed by Bontrager (Ref. 1) and others (Refs. 4 and 5) was undertaken. An analysis was made of the differences, similarities, and problem areas of the three correction methods. A new approach to the total temperature probe correction was developed in an attempt to account for the shortcomings of these previous methods. The analysis is based on the total temperature variation in a laminar developing flow within a tube whose walls are at the adiabatic recovery temperature of the local flow field. This approach results in the ability to theoretically correct probe data for all local flow-field conditions with calibration data only required in the free stream. Corrections made to total temperature measurements by this new method are compared to theoretical predictions and reveal a significant improvement over previous approaches.

2.0 DISCUSSION OF PRESENT METHODS

The total temperature probe currently in use at AEDC-VKF evolved from the need for a probe that would give accurate and consistent results and at the same time be both rugged and relatively easy to manufacture. Figure 1 is a sketch of the probe showing the important physical dimensions. Recent tests have employed probes of varying size depending mostly upon test requirements. Typical configurations that have been used are presented in Table 1.

The parametric study conducted by Bontrager (Ref. 1) was used to define the best compromise of probe geometry in order to reduce the cumulative errors attributable to radiation, velocity, and conduction. The radiation error results principally from the inability of the probe shield to block energy radiated to the "cold" tunnel walls. Bontrager examined the case when the tunnel flow was neither an emitter nor an absorber and concluded that the radiation error could be neglected when compared to the convection losses. Velocity error

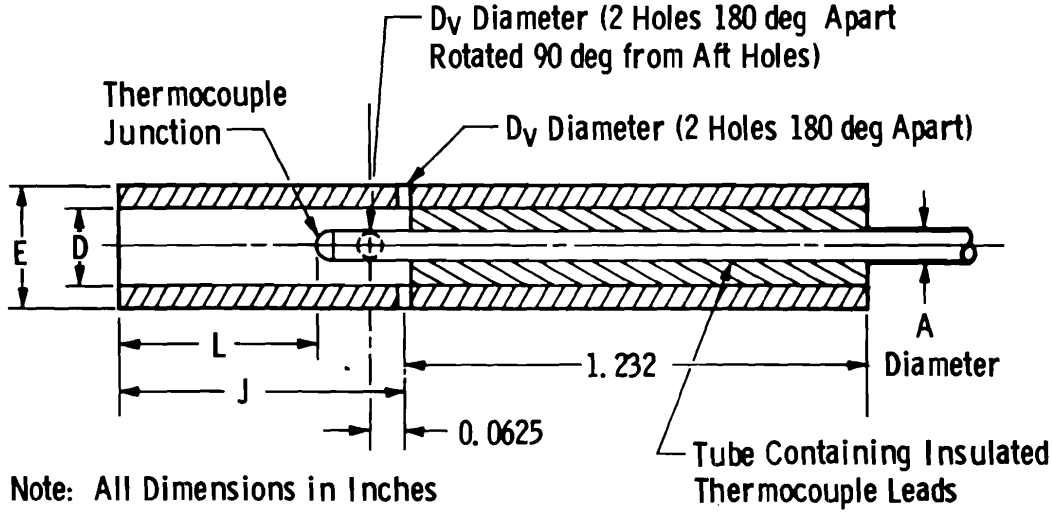

Figure 1. Schematic of single-shielded, total temperature probe.

Table 1 Typical Values of Geometric Parameters for Probe Shown in Fig. 1

Configuration	A	D	E	D_V	J	L
1	0.010	0.034	0.038	0.012	0.427	0.068
2	0.020	0.056	0.060	0.020	0.668	0.112
3	0.020	0.076	0.080	0.027	0.728	0.152
4	0.040	0.144	0.156	0.051	1.032	0.288

resulted from the inability of the thermocouple junction to recover all of the kinetic energy of the flowing gas within the probe. For mean probe Mach numbers of 0.3 or less, the velocity error was shown to be less than 0.25 percent. Heat conduction along the thermoelectric wires was considered by modeling the thermocouple wire as an extended surface. For relative high length-to-diameter ratios of the wire, conduction effects were shown to be negligible.

Bontrager's analysis indicated that probe entrance length-to-diameter ratios of 2.0, entrance area-to-vent area ratios of 2 or greater, and exposed wire lengths much greater than the wire diameter would result in total temperature measurements essentially free of conduction, radiation, and velocity errors. Probes considered here are assumed to adhere to these restrictions, and, thus, the effect of these errors on the total temperature probe correction will not be considered further.

The largest single factor affecting the ratio of measured-to-actual total temperature is the loss in energy associated with the developing thermal boundary layer in the entrance region of the probe. Thus, Bontrager attemped to correlate the ratio of measured-to-actual temperature with the products of Reynolds number, Re_D, based upon conditions at the probe entrance, where

$$Re_D = \left[\left(\frac{2}{\gamma + 1}\right)^{1/\gamma - 1}\left(\frac{2\gamma}{\gamma + 1}\right)^{1/2}\frac{1}{R^{1/2}}\right]\frac{A_v}{A_e}\;\frac{p_{o_e} D}{\mu_e T_{o_i}^{1/2}} \qquad (1)$$

and the ratio D/L. Here A_v/A_e is the vent area-to-entrance area ratio, p_{o_e} is the pitot pressure at the total temperature probe location, D is the probe internal diameter (ID), L is the distance from the probe entrance to the thermocouple junction, μ_e is the absolute viscosity based on entrance conditions, and T_{o_i} is the local total temperature. The specific heat ratio, γ, is approximately constant

over the temperature range of interest, and R is the gas constant. The functional form of Re_D as expressed in Eq. (1) assumes choked flow through the probe vent areas (see Fig. 1). For constant Mach number conditions, calibration data appeared to correlate Re_D with the measured-to-actual total temperature ratio (T_{o_m}/T_{o_i}).

The main error in Bontrager's correlation is the neglect of the loss of thermal energy associated with the local undisturbed flow at Mach number M_i. In an attempt to account for the loss in kinetic energy of the flow when brought to rest, a recovery factor of the probe has been defined and used in numerous studies (for example, see Refs. 2 and 3). For a flow brought to rest adiabatically,

$$T_{o_i} = T_i \left(1 + \frac{\gamma - 1}{2} M_i^2\right) \tag{2}$$

For a nonadiabatic flow, a recovery factor, η, may be defined, in conventional terms, by

$$T_{o_m} = T_i \left(1 + \eta \frac{\gamma - 1}{2} M_i^2\right) \tag{3}$$

where T_{o_m} is the measured total temperature. Eliminating T_i from Eqs. (2) and (3) and solving for η, one derives Eq. (4):

$$\eta = \frac{\left(T_{o_m}/T_{o_i}\right)\left(1 + \frac{\gamma - 1}{2} M_i^2\right) - 1}{\frac{\gamma - 1}{2} M_i^2} \tag{4}$$

Equation (4) has been used extensively as a correlation parameter against Re_D for a fixed probe geometry.

Recently, Laderman (Ref. 4) used the definition of η given in Eq. (4) to correlate the total temperature correction with the local Reynolds number, $\acute{Re}_D$, based on the probe diameter, local unit mass flow, and local total temperature. The similarity of the present shielded probe with an unshielded thermocouple probe suggested this particular correction procedure. Even though this method does attempt to account for the Mach number effect, correlation of η with the

local Reynolds number overlooks the area change of the stream tube captured by the probe because of changes in the local flow condition (for instance, through a boundary layer). Some typical calculations have been made that indicate, for a fixed probe geometry, variations of up to 100 percent in the diameter of the stream tube captured exist for a probe traverse through a 4-deg cone boundary layer at Mach 10.

By a somewhat similar analysis, Martellucci (Ref. 5) has used the unit mass flow through the probe versus η for correcting total temperature measurements. By using this unit mass flow, the problem encountered in Laderman's method is eliminated. The use of unit mass flow as a correlation parameter neglects, however, viscous effects in the entrance region of the probe for length-to-diameter (L/D) values different from zero. Moreover, for a typical flow-field survey as mentioned in the previous paragraph, the absolute viscosity of the flow in the entrance region of a probe can change by as much as 30 percent. Thus, the methods of Laderman and Martellucci (Refs. 4 and 5, respectively) effectively deal with portions of the correction problem but fail to handle the entire problem adequately.

An additional serious deficiency that pervades all the previously mentioned methods is the fact that probe calibrations are made in flow environments considerably different, as a general rule, from the environment over which the corrections are applied. Typical calibrations of total temperature probes in Tunnel C generally cover an Re_D range of 100 to 1,000. Over this Re_D range η is well defined. For values of Re_D less than the lower limit of the calibration data, considerable uncertainty exists in the shape and magnitude of the η versus Re_D curve. Moreover, it is not clear that the definition of η properly accounts for the Mach number effect.

In order to assess the magnitude of these uncertainties, some sample calculations were made. Calibration curves based on each of

the three methods were allowed to vary between reasonable limits outside the range of the calibration data. These curves were then applied to the correction of total temperature measurements in the laminar boundary layer of a 4-deg sharp cone at Mach 10 in Tunnel C. Possible errors in the corrected measurements of 10 to 100 percent resulted. These variations are, of course, extreme and may be reduced by a more precise definition of the calibration curve. The variations are, however, reasonable in light of present calibration procedures.

3.0 IMPROVED CORRECTION METHOD

The previous sections have examined the problems associated with three methods [those of Bontrager, (Ref. 1), Martellucci (Ref. 5), and Laderman (Ref. 4)] in defining an accurate correction to total temperature measurements made with the single-shielded, thermocouple probe. Deficiencies have been shown to exist in these methods which may result in large errors in the corrected T_o measurement. The purpose of this section will be the development of an improved correction method that effectively eliminates these major sources of error.

Consider the flow and geometric model as shown in Fig. 2. Assume that the vent flow is choked over the entire Mach number calibration and correction range. The developing flow in the entrance region of the probe is assumed to be laminar for all entry Reynolds numbers based on the distance to the thermocouple junction and to be unaffected by thermal gradients. A developing thermal layer exists because of the heat flux resulting from the difference in the temperature of the entering flow (e) and in the adiabatic recovery temperature of the shield based on local conditions (i). The size of the thermocouple junction relative to the internal area of the shield ($\pi D^2/4$) is assumed to be small enough so that it does not affect the flow field within the tube. Then, by defining the function g as

$$g = \frac{T - T_s}{T_e - T_s} \tag{5}$$

where T is the local centerline temperature within the probe and where T_e and T_s are the entering temperature of the flow and the adiabatic recovery temperature of the shield, respectively, the functional form of the measured-to-actual total temperature may be determined. Hence,

$$\frac{T_{o_m}}{T_{o_i}} = 1 + (g - 1)(T_e - T_s)/T_{o_i} + \frac{\gamma R}{2c_p} \frac{T_e M_e^2}{T_{o_i}} \left[\left(\frac{u}{u_e}\right)^2 - 1\right] \qquad (6)$$

Here c_p is the specific heat at constant pressure. The terms M_e and u/u_e are the entrance Mach number and ratio of centerline axial velocity at the thermocouple junction to the axial entrance velocity, respectively. For choked vent flow, the ratio of entrance flow area, A_e, to effective vent flow area, A_v, defines the entrance Mach number for isentropic flow. Equation (6), of course, implies no losses in bringing the flow to rest at the thermocouple junction. This error is negligible for all practical flow geometries considered.

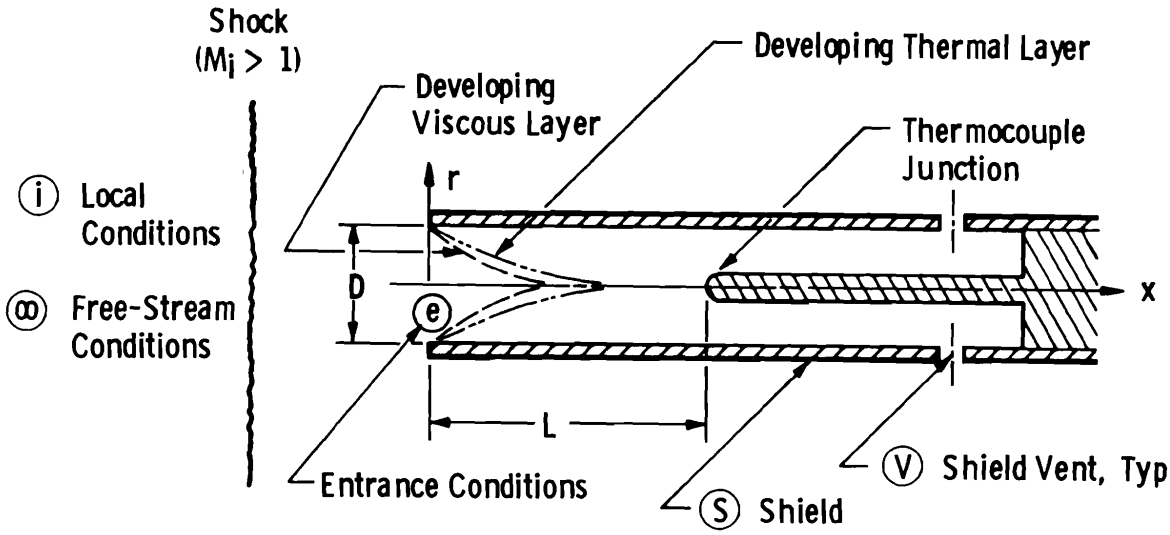

Figure 2. Typical probe showing parameters of importance.

Employing the conventional definition of the recovery temperature of the shield, one may refine Eq. (6) to give

$$\frac{T_{o_m}}{T_{o_i}} = 1 + (g - 1)\,\Gamma(M_i; M_e, R^*) + \frac{\gamma R}{2c_p}\frac{T_e}{T_{o_i}} M_e^2 \left[\left(\frac{u}{u_e}\right)^2 - 1\right] \tag{7}$$

where

$$\Gamma(M_i; M_e, R^*) = \left[T_e/T_i - \left(1 + \frac{\gamma - 1}{2} R^* M_i^2\right)\right] T_i/T_{o_i} \tag{8}$$

The use of the isentropic flow relations allows for the definition of T_e/T_i and T_i/T_{oi} assuming M_e and M_i are known. The recovery factor of the shield, R*, is equal to $Pr^{1/2}$ for laminar flow where Pr is the Prandtl number of the local flow field. Figure 3 shows the influence of the recovery factor on Γ as a function of the local Mach number. From this figure it may be seen that, for fixed M_i and g, increasing R* tends to decrease the effect of the local Mach number on the temperature correction. The variation of Γ with M_i for R* equal to 0.84 is shown in Fig. 4, indicating the limiting nature of Γ for increasing values of A_e/A_v.

The only quantities not yet defined in Eq. (7) are the function g and the velocity ratio u/u_e. It is appropriate here to discuss the possible forms of g and their dependence on the flow field within the probe. A comparison of various solutions will be made first, followed by a brief presentation of the functional form of the solutions. Figure 5 shows a total of five solutions for g that depend on the Peclet number, Pé, which is equal to $Re_D Pr/2$, and the ratio L/D. Generally, for all values of L/D, g is bounded by the values 0 and 1, asymptotically approaches these limits as Pé approaches 0, and grows without bound. A comparison of similar curves for different L/D values indicates a functional shift of the g curve with Pé. An examination of the effects of axial heat conduction reveals their importance for Peclet numbers less than 20. The trends of g versus Peclet number for comparable fully developed laminar and potential

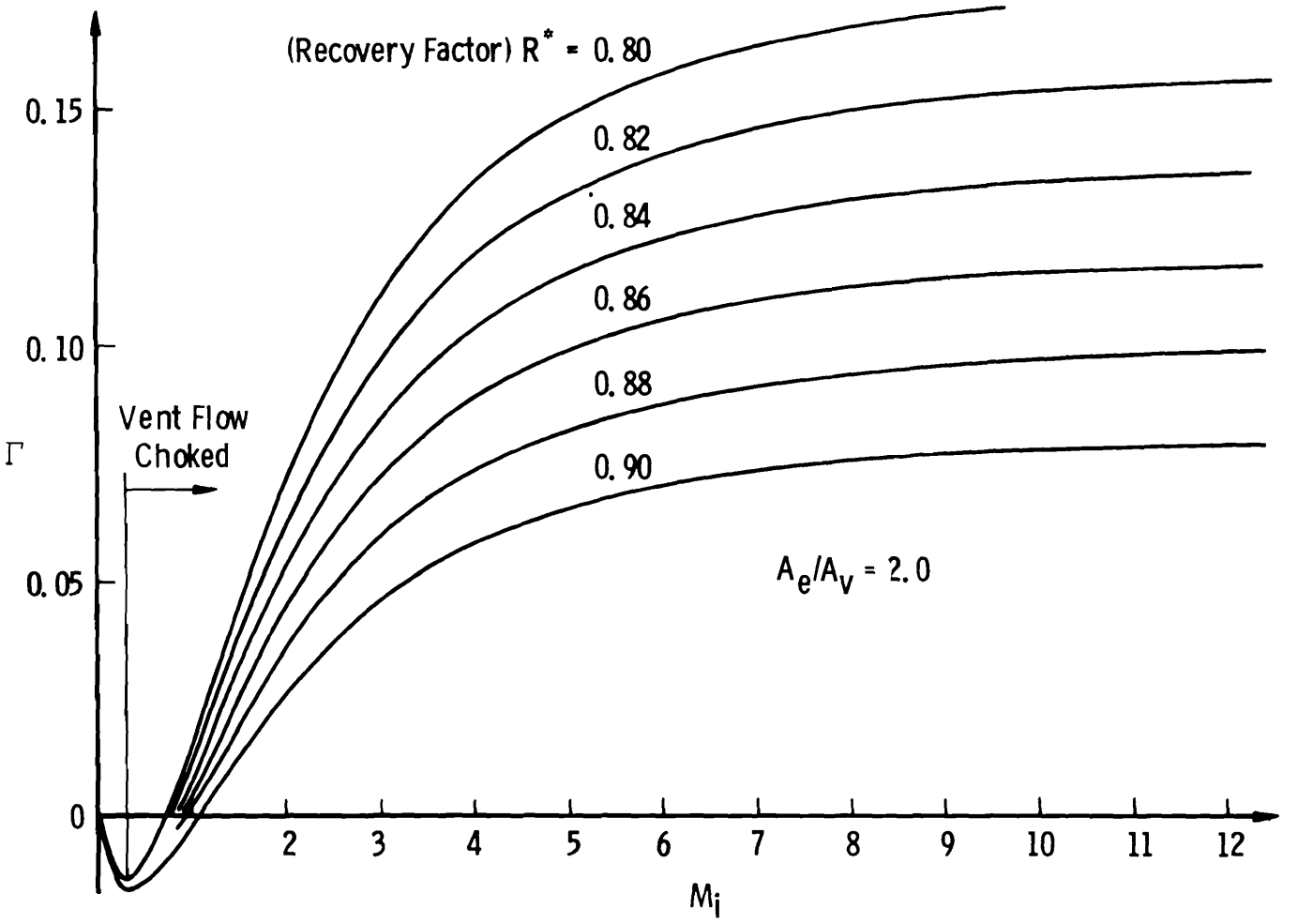

Figure 3. Gamma versus local Mach number for fixed A_e/A_v showing effect of probe shield recovery factor.

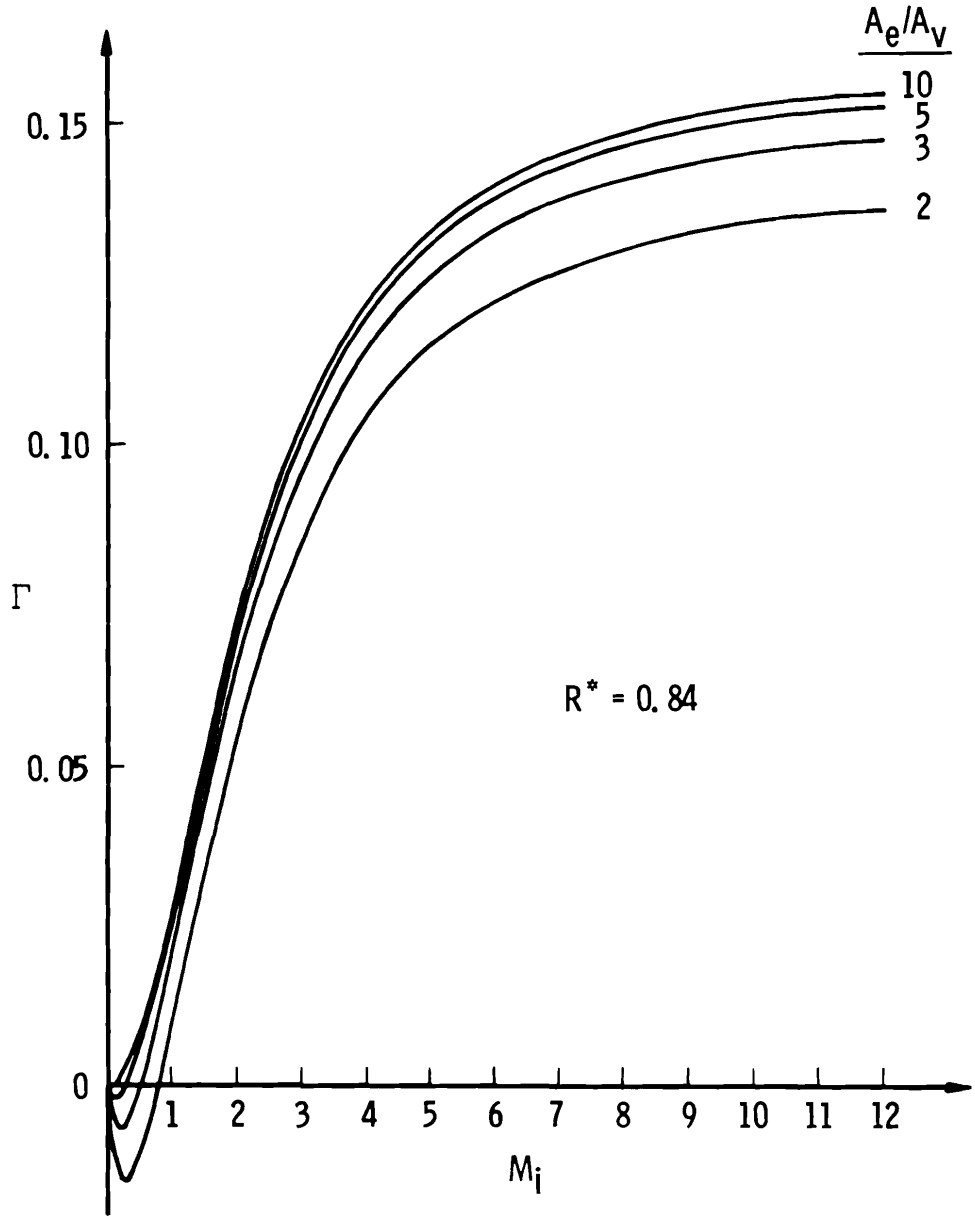

Figure 4. Gamma versus local Mach number for fixed probe recovery factor showing effect of A_e/A_v.

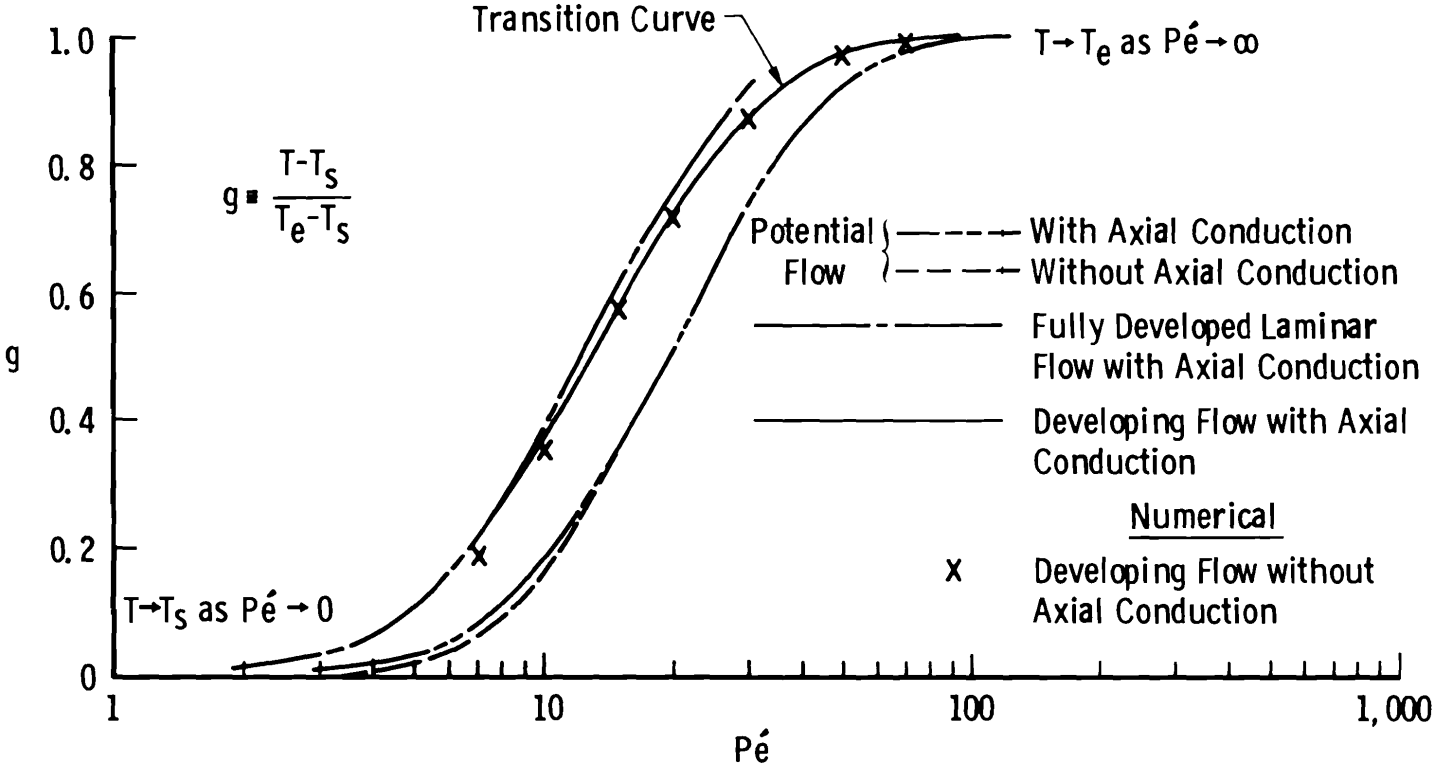

Figure 5. Temperature distribution along probe centerline as a function of Peclet number for L/D = 2.0.

flows also suggests a functional shift of the g curve for a given L/D value. The variation of g with $P\acute{e}$ and L/D was evaluated numerically for a developing flow in the entrance length of the probe for the case with no axial conduction. In the limits, the developing flow solution tends to fully developed laminar and potential solutions for $P\acute{e}$ approaching 0 and for $P\acute{e}$ approaching infinity, respectively. Included in these figures is a transition curve derived by shifting the developing flow solution an amount equal to the difference in the potential flow solutions with and without axial conduction. Thus, the required g curve to be used in Eq. (7) for the total temperature correction is the transition curve coupled with the developing flow solution for u/u_e.

The five basic solutions were derived from the governing energy equation for axisymmetric, steady flow in the axial direction only. The effect of the radial velocity component in the entrance region of the probe on the thermal layer solution is neglected since $P\acute{e}$ is generally less than 300 (Ref. 6). The effect of the axial velocity gradient in the radial direction has also been assumed negligible. The boundary conditions and governing equation in terms of the function g and $\omega = r/r_o$ and $x' = x/(r_o P\acute{e})$ are given in Eqs. (9) and (10) with coordinates as illustrated in Fig. 2; here r_o is the tube radius equal to D/2.

$$\frac{u}{u_e}\frac{\partial g}{\partial x'} = \frac{1}{P_e'^2}\frac{\partial^2 g}{\partial x'^2} + \frac{1}{\omega}\frac{\partial}{\partial \omega}\left(\omega \frac{\partial g}{\partial \omega}\right) \tag{9}$$

$$\begin{aligned} \text{B. C.:}\quad & g = 0 \text{ for } x' > 0,\ \omega = 1 \\ & g = 1 \text{ for } x' = 0,\ 0 < \omega \leq 1 \\ & g \to 0 \text{ as } x' \to \infty \end{aligned} \tag{10}$$

An exact solution to Eq. (9) subject to the boundary conditions given in Eq. (10) is possible for the case where $u/u_e = 1.0$ (potential flow).

The solution may be expressed in the form of Eq. (11) for the cases considered, neglecting axial conduction represented by the term

$$g = \sum_{n=1}^{\infty} \frac{2}{\alpha_n J_1(\alpha_n)} \exp(-\beta_n^2) J_0(\alpha_n \omega) \tag{11}$$

where

$$\beta_n^2 = \alpha_n^2 \frac{2}{P_e'} \left(\frac{L}{D}\right) \tag{12}$$

neglecting axial conduction (Ref. 7) and

$$\beta_n^2 = \left(\frac{L}{D}\right)\left[\left(P\acute{e}^2 + 4\alpha_n^2\right)^{1/2} - P\acute{e}\right] \tag{13}$$

including axial conduction (Ref. 8). J_0 and J_1 are Bessel functions of the first kind of order zero and one, respectively, and α_n are the zeros of $J_0(\alpha_n)$. An approximate analytic solution for the fully developed laminar case including axial conduction (Ref. 8) is also shown to be expressed by Eq. (11) with, however,

$$\beta_n^2 = 2\left(\frac{L}{D}\right)P\acute{e}\left\{\left[\frac{4}{9}\left(1 + \frac{1}{\alpha_n^2}\right)^2 + \frac{\alpha_n^2}{P\acute{e}^2}\right]^{1/2} - \frac{2}{3}\left(1 + \frac{1}{\alpha_n^2}\right)\right\} \tag{14}$$

where $u/u_e = 2(1 - \omega^2)$. It is important to note that the three solutions can all be expressed in the form

$$g = \sum_{n=1}^{\infty} C_n \exp\left[-\left(\frac{L}{D}\right) q\left(P\acute{e}, \alpha_n\right)\right] \tag{15}$$

for $\omega = 0$, where the C_n are constants and q is a function of $P\acute{e}$ and α_n only. This similarity reinforces the observation made earlier that the effect of a given change in L/D is to shift the g curve with respect to Peclet number by approximately a constant.

The numerical evaluation of the case for developing flow neglecting axial conduction effects follows Kays (Ref. 9), employing, however, the solution of Sparrow, Lin, and Lundgren (Ref. 10) for the

hydrodynamic flow development in the entrance region of the tube. The axial velocity distribution within the tube is given in Eq. (16):

$$\frac{u}{u_e} = 2(1 - \omega^2) + \sum_{n=1}^{\infty} \frac{4}{\alpha_n^2} \left[\frac{J_0(\alpha_n \omega)}{J_0(\alpha_n)} - 1 \right] \exp(-\alpha_n^2 x^*) \tag{16}$$

where x* is evaluated by

$$Prx' = \int_0^{x^*} \epsilon \, d x^* \tag{17}$$

and ε is given by

$$\epsilon = \frac{\int_0^1 \left[2\left(\frac{u}{u_e}\right) - 1.5\left(\frac{u}{u_e}\right)^2 \right] \frac{\partial\left(\frac{u}{u_e}\right)}{\partial x^*} \omega \, d\omega}{\left.\frac{\partial\left(\frac{u}{u_e}\right)}{\partial \omega}\right|_{\omega=1} + \int_0^1 \left[\frac{\partial\left(\frac{u}{u_e}\right)}{\partial \omega}\right]^2 \omega \, d\omega} \tag{18}$$

Equation (18) has been evaluated numerically and is given in Fig. 6 for $x^* \leq 0.20$. For values of x* greater than 0.20, ε is approximately constant and equal to 1.82. Figure 7 is a plot of the axial velocity ratio along the tube centerline as a function of $Re_D/(L/D)$.

Using the expression for the velocity ratio given in Eq. (16), the governing energy equation was solved numerically for the case of no axial conduction. For the interior grid points

$$g_{i+1,j} = f_1 g_{i,j+1} + f_2 g_{i,j} + f_3 g_{i,j-1} \tag{19}$$

where

$$\begin{aligned} f_1 &= \left(\frac{u_e}{u}\right)\left(\frac{\Delta x'}{\Delta \omega}\right)\left[\frac{1}{\Delta \omega} + \frac{1}{2\omega}\right] \\ f_2 &= 1 - 2\left(\frac{u_e}{u}\right)\left(\frac{\Delta x'}{\Delta \omega^2}\right) \\ f_3 &= \left(\frac{u_e}{u}\right)\left(\frac{\Delta x'}{\Delta \omega}\right)\left[\frac{1}{\Delta \omega} - \frac{1}{2\omega}\right] \end{aligned} \tag{20}$$

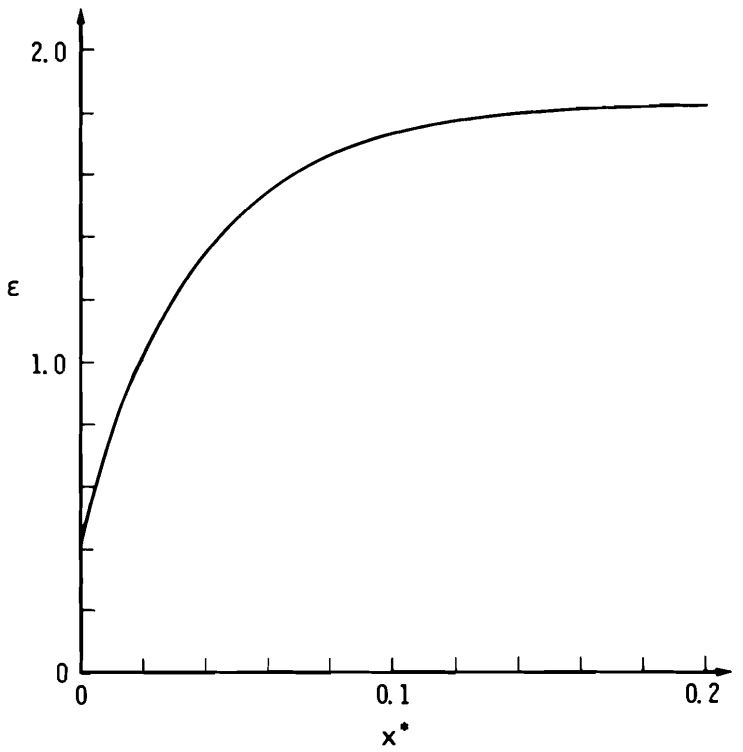

Figure 6. Variation of ϵ with x* for developing tube flow.

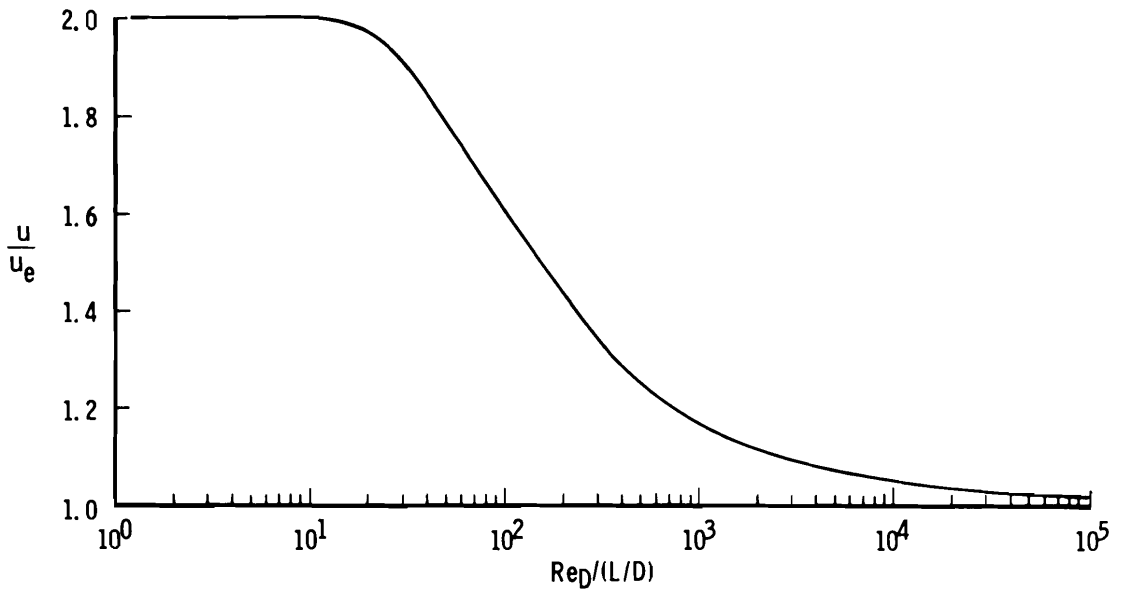

Figure 7. Axial velocity ratio along tube centerline in hydrodynamic entrance region.

Here $\Delta x'$ and $\Delta\omega$ are the grid spacings in the axial (i) and radial (j) directions, respectively. Along the tube centerline,

$$g_{i+1,1} = f_2\, g_{i,1} + \frac{2u_e}{u}\frac{\Delta x'}{\Delta\omega^2}\, g_{i,2} \tag{21}$$

and at the boundaries,

$$\begin{aligned} g &= 0 \text{ at } \omega = 1,\ x' \geq 0 \\ g &= 1 \text{ at } x' = 0,\ 0 \leq \omega < 1 \end{aligned} \tag{22}$$

Typical velocity and temperature profiles are shown in Fig. 8. The general solution for g as a function of Pé and L/D along the tube centerline is shown in Fig. 9 with the axial conduction effect included. Thus, with the definition of u/u_e and g as a function of Pé, Re_D, and L/D, an improved calibration and correction of total temperature probe data may be obtained through the use of Eqs. (7) and (8).

4.0 DISCUSSION AND CONCLUSIONS

The preceding section has presented a new method for the correction of total temperature measurements made with a single-shielded, thermocouple probe. A discussion of some of the important characteristics and their relationship to previous methods (Refs. 1, 4, and 5) will aid in an understanding of the applicability of the new technique.

An application of the new method to some laminar flow data from a recent test in Tunnel C is given in Figs. 10 through 13. The total temperature probe used had nominal dimensions corresponding to configuration 2 as listed in Table 1. The experimental calibration data were obtained in the free stream by varying the tunnel stagnation pressure. The data were used to determine the experimental value of the vent ratio. Figure 10 shows the fit of the g curve through the calibration data for the experimental value of A_v/A_e of 0.11. The experimental data scatter about the g curve is equivalent to a maximum error in T_{o_m}/T_{o_i} of the theory compared to the calibration data of ±0.5 percent.

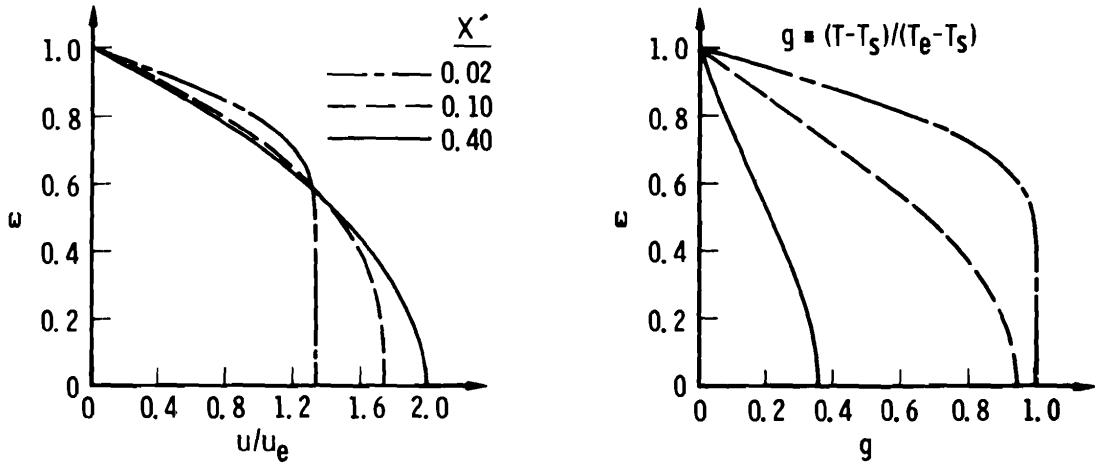

Figure 8. Typical radial velocity and temperature profiles for Pe' = 10.0 and Pr = 0.7.

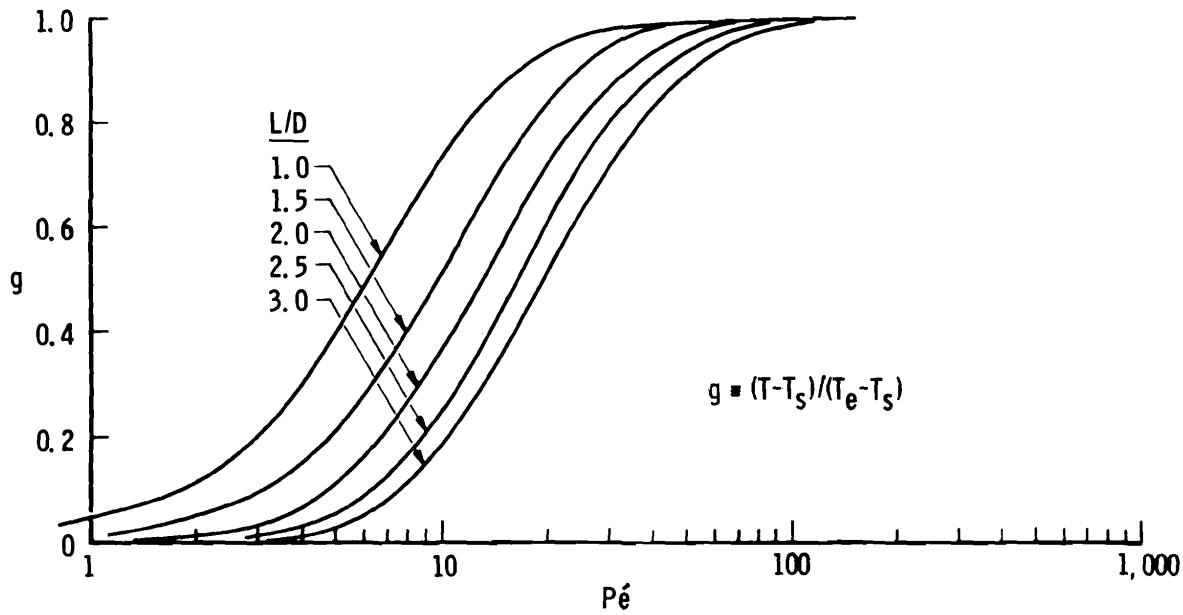

Figure 9. Temperature distribution along probe centerline as a function of Peclet number for developing flow with axial conduction.

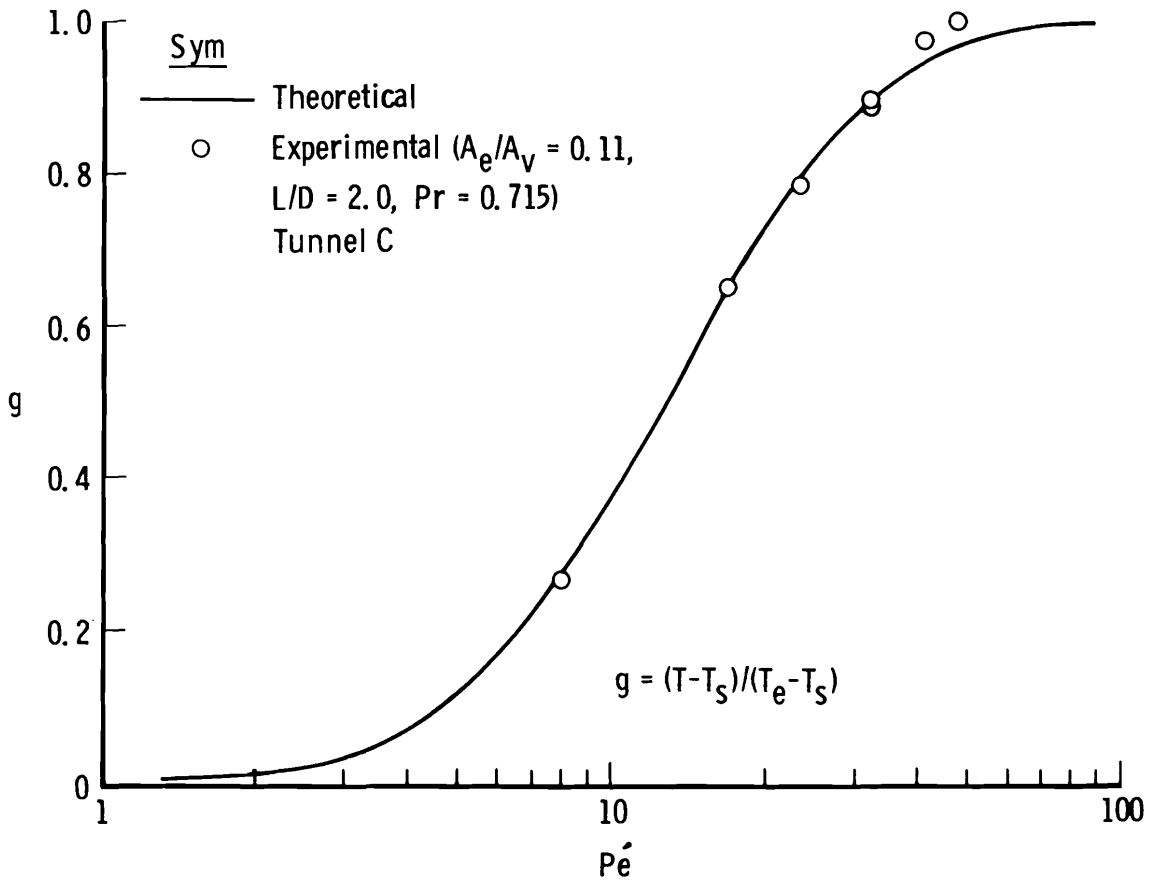

Figure 10. Calibration curve for improved method.

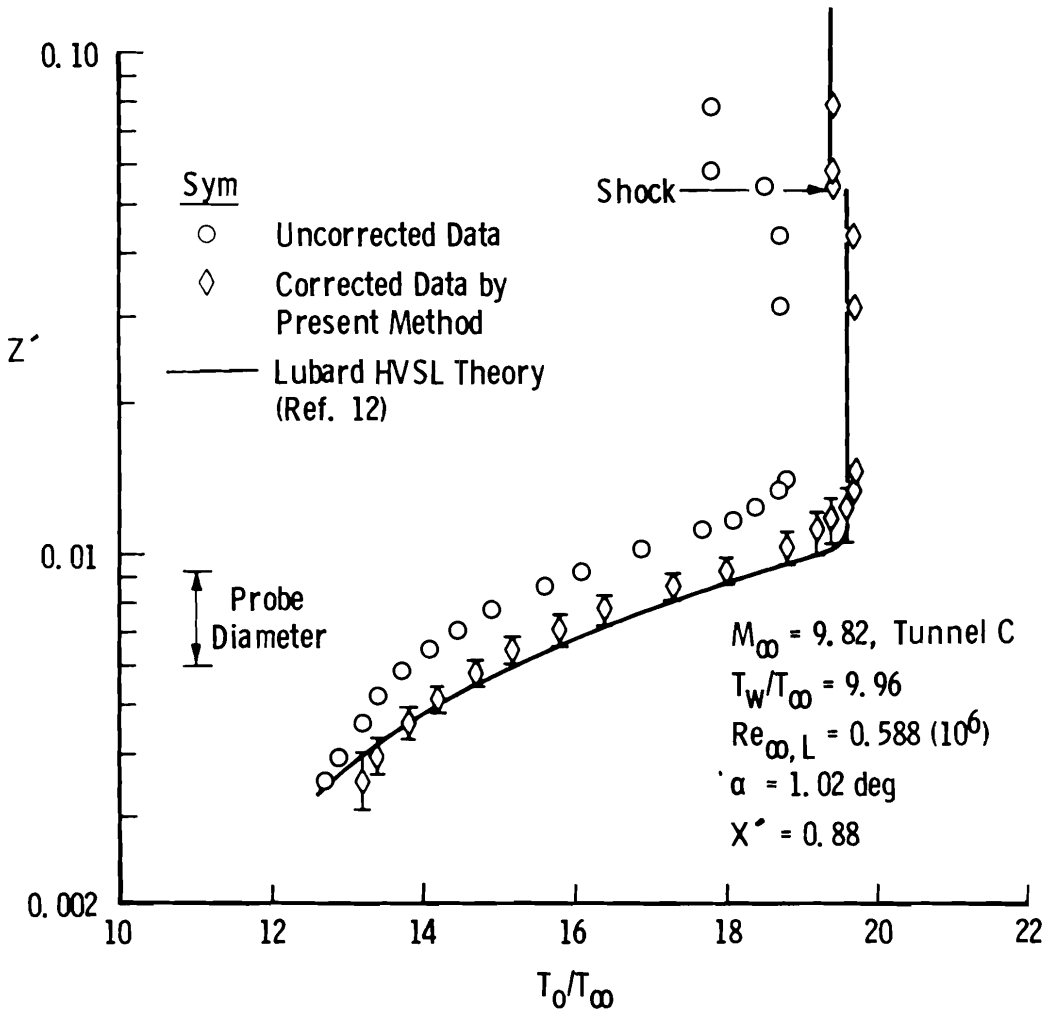

Figure 11. Comparison of the corrected experimental and theoretical total temperature within the boundary layer of a 4-deg cone at low $Re_{\infty L}$.

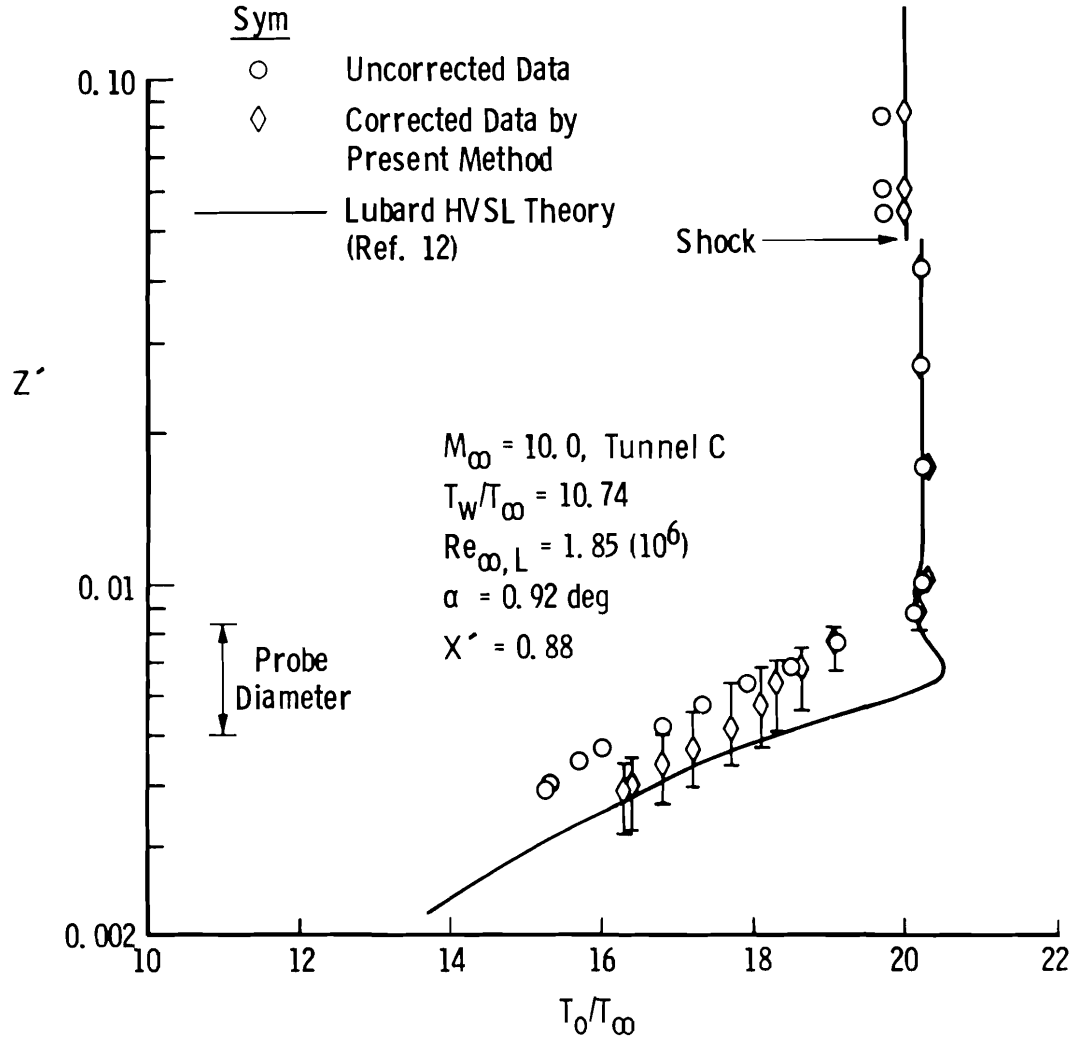

Figure 12. Comparison of the corrected experimental and theoretical total temperature within the boundary layer of a 4-deg cone at moderate $Re_{\infty L}$.

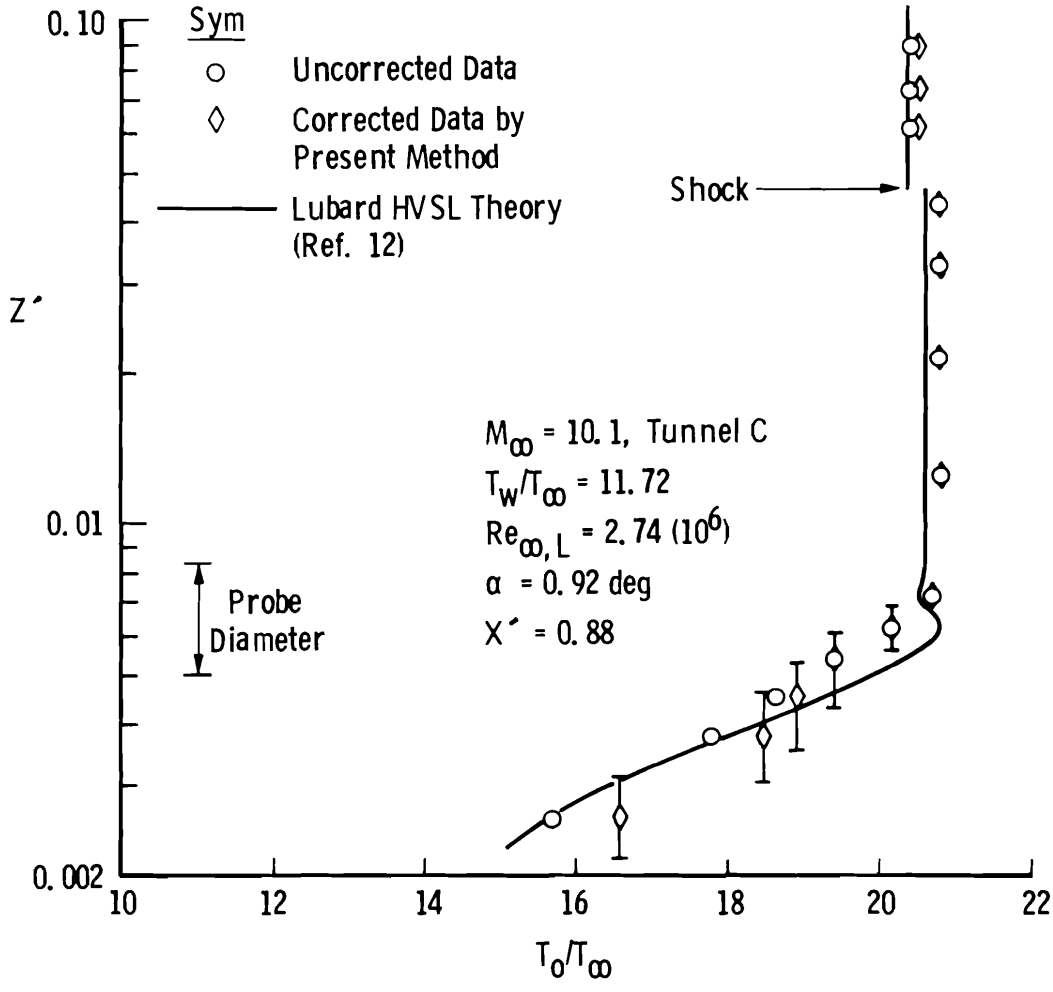

Figure 13. Comparison of the corrected experimental and theoretical total temperature within the boundary layer of a 4-deg cone at high $Re_{\infty L}$.

In general, the vent area ratio is a function of the pressure ratio, p_i/p_{o_e}, and the vent Reynolds number, Re_v (see Ref. 11). This effect has been included in the present correction procedure. For the calibration and flow-field data considered here, the variation of A_v/A_e with Re_v and p_i/p_{o_e} was insignificant. For smaller probes, however, this effect will become important. A post-test bench calibration of the probe gave $A_v/A_e = 0.14$. The low experimental value as compared to $A_v/A_e = 0.5$ obtained from Table 1 is caused by the partial restriction of the vent holes during construction. The character of the mean flow over the vent holes was expected to be a significant parameter in determining the effective vent flow area. The difference in the value of A_v/A_e obtained by calibration in the tunnel and by the bench calibration (correcting for relative Re_v and p_i/p_{o_e}) was felt to be representative of this effect and the difference was assumed constant for the local flow-field conditions considered.

Measurements were taken at an axial station of 0.88 of the model length measured from the nose on the windward ray of a 4-deg sharp cone at a nominal angle of attack of 1 deg and Mach number of 10. All distances referred to in Figs. 11, 12, and 13 have been nondimensionalized by the model axial length.

Figure 11 shows the uncorrected and corrected total temperature data as a function of the Z´ coordinate measured normal to the cone surface at a Reynolds number based on total model length ($Re_{\infty,L}$) of 0.588×10^6 and wall temperature ratio of $T_w/T_\infty = 9.96$. The band on the corrected data represents a probe location uncertainty of ±0.0006 in Z´. For comparison purposes, the hypersonic viscous shock layer (HVSL) theory of Ref. 12 is also shown in Fig. 11 for identical free-stream conditions. The theoretical total temperature profiles were computed using an "effective" c_p based on the average of the local static and stagnation temperatures. The corrected data are seen to be in excellent agreement with the theory. This is indirect verification of the present

method since there were large variations within the boundary layer of Re_D (from 1.5 to 50) and M_i (from 1.2 to 9.82) compared to the calibration conditions of $23 < Re_D < 120$ and $M_\infty = 10$. Also indicated in the figure is the relative size of the probe. Considering the probe size effect near the wall and at the knee in the T_o/T_∞ profile, the corrected data also exhibit the proper trends.

Figures 12 and 13 give a comparison of the corrected data and theory for $Re_{\infty,L} = 1.85 \times 10^6$, $T_w/T_\infty = 10.74$ and $Re_{\infty,L} = 2.74 \times 10^6$, $T_w/T_\infty = 11.72$, respectively. Agreement here is seen to be good in both magnitude and expected trend. The effect of probe size on the measured data for these higher Reynods number conditions when compared to Fig. 11 is greater at the knee of the total temperature profile because of the steeper temperature gradient. Thus, the present correction results in very good total temperature correlation between experiment and theory.

An interesting aspect of the new correction method is its relationship to the methods of Laderman and Martellucci (Refs. 4 and 5, respectively). If the total temperature correction equation, Eq. (7), is rewritten using Eq. (4) with η as defined in Refs. 4 and 5, the correction equation may be reduced to the following form:

$$\eta = 1 + (g-1)\Gamma' + \frac{\gamma R}{2c_p}\frac{T_e}{T_{o_i}} M_e^2 \left[\left(\frac{u}{u_e}\right)^2 - 1\right] \Big/ \left(1 - T_i/T_{o_i}\right) \qquad (23)$$

where

$$\Gamma' = \Gamma/(1 - T_i/T_{o_i}) \qquad (24)$$

For very large values of A_e/A_v (on the order of 10 or greater) and local Mach numbers much larger than 1, the contribution of the term representing kinetic energy of the developing flow within the tube in Eq. (23) may be neglected and Γ' is approximately constant. Thus, η becomes a function of Re_D and L/D only. This result agrees with the

form of η used by Laderman and Martellucci. As the entrance area-to-vent area ratio is decreased, however, the kinetic energy term increases in magnitude and may not be neglected. Moreover, Γ' may no longer be assumed independent of M_i.

In some of Bontrager's experimental results, there is a definite "overshoot" of the calibration curve above 1.0. Bontrager could not account for the magnitude of this overshoot. The form of the new correction as given in Eq. (7) does allow for an overshoot in T_{o_m}/T_{o_i} that is predominantly influenced by the value of A_e/A_v. For example, under free-stream calibration conditions ($Re_D > 200$) with L/D = 2, values of A_e/A_v on the order of two are required to give a two-percent overshoot in T_{o_m}/T_{o_i}. Another feature of the new method when compared to the previous methods applied to the calibration and correction of total temperature probe data is the fact that the new method has a lower limit on T_{o_m}/T_{o_i}. For a given probe configuration, the limit is approximately equal to $1 - \Gamma_{max}$ for large values of A_e/A_v and occurs when $T = T_e$.

In conclusion, methods of total temperature correction for a single-shielded, thermocouple probe have been examined. The important problems associated with each method have been addressed. Because of the inability of any one of the earlier methods to handle satisfactorily the correction problem, a new method was developed based on a detailed examination of the developing thermal layer within the tube. The theoretical form of the solution allows for total temperature corrections to be made in an uncalibrated Mach number and/or local Reynolds number region. This new correction method appears to be a significant improvement over previous approaches.

REFERENCES

1. Bontrager, P. J. "Development of Thermocouple-Type Total Temperature Probes in the Hypersonic Flow Regime." AEDC-TR-69-25 (AD681489), January 1969.

2. Winkler, E. M. "Stagnation Temperature Probes for Use at High Supersonic Speeds and Elevated Temperatures." NAVORD Report 3834, October 1954.

3. Voisinet, R. L. P., Lee, R. E., and Meier, H. U. "Comparative Measurements of the Total Temperature in a Supersonic Turbulent Boundary Layer Using a Conical Equilibrium and Combined Temperature-Pressure Probe." NOL TR-74-10, July 1974.

4. Laderman, A. J. "Effect of Mass Addition and Angle-of-Attack on the Hypersonic Boundary Layer Turbulence Over a Slender Body." Philco-Ford Corp. Publication No. U6047, September 1972.

5. Martellucci, A., Laganelli, A., and Hahn, J. "Hypersonic Turbulent Boundary Layer Characteristics with Mass Transfer, Volume 1." SAMSO TR-74-112, April 1974.

6. Ulrichson, D. L. and Schmitz, R. A. "Laminar-Flow Heat Transfer in the Entrance Region of Circular Tubes." International Journal of Heat and Mass Transfer, Vol. 8, 1965, pp. 253-258.

7. Jakob, Max. Heat Transfer. Vol. 1, John Wiley and Sons, N. Y., 1958, pp. 451-459.

8. Singh, S. N. "Heat Transfer by Laminar Flow in a Cylinderical Tube." Applied Scientific Research, Section A, Vol. 7, 1957-1958, pp. 325-340.

9. Kays, W. M. Numerical Solutions for Laminar-Flow Heat Transfer in Circular Tubes." Transactions of the ASME, November 1955, pp. 1265-1274.

10. Sparrow, E. M., Lin, S. H., and Lundgren, T. S. "Flow Development in the Hydrodynamic Entrance Region of Tubes and Ducts." The Physics of Fluids, Vol. 7, No. 3, March 1964, pp. 338-347.

11. Smetana, Fredrick O., Sherrill, W. A., II, and Schort, Donald R., Jr. "Measurement of the Discharge Characteristics of Sharp-Edged and Round-Edge Orifices in the Transition Regime." 5th International Symposium on Rarefied Gas Dynamics, Proceedings, Oxford, England, Vol. 2, 1967, pp. 1243-1256.

12. Lubard, Stephen C. and Helliwell, Willaim S. "Calculation of the Flow on a Cone at High Angles of Attack." RDA-TR-150, February 1973.

NOMENCLATURE

A	Flow area
C_n	Series constants
c_p	Specific heat at constant pressure
D	Probe entrance diameter

D_v	Probe vent hole diameter
f_1, f_2, f_3	Functions as given in Eq. (20)
g	Function equal to $(T - T_s)/(T_e - T_s)$
L	Entrance length to thermocouple junction
M	Mach number
n	Integer
Pé	Peclet number equal to $PrRe_D/2$
Pr	Prandtl number
p	Pressure
p_o	Total pressure
q	Function of Pé and α_n
R	Gas constant
R*	Recovery factor of the shield
Re_D	Reynolds number based on probe entrance condition
$Ré_D$	Reynolds number based on local condition and probe entrance diameter
Re_v	Probe vent Reynolds number

$Re_{\infty,L}$	Free-stream Reynolds number based on cone model length
r	Radial coordinate as shown in Fig. 2
r_o	Probe entrance radius
T	Temperature
T_o	Total temperature
u	Axial velocity
x	Axial coordinate as shown in Fig. 2
x'	Dimensionless axial coordinate
x*	Stretched dimensionless axial coordinate
Z'	Dimensionless surface normal coordinate
α	Angle of attack
α_n	Eigenvalues equal to zero's of $J_0(\alpha_n)$
β_n	Function of α_n and $\acute{Pe}$ as given in Eqs. (12), (13), and (14)
Γ	Function as defined in Eq. (8)
Γ'	Function as defined in Eq. (24)
γ	Specific heat ratio

$\Delta x'$ Grid spacing in x' direction

$\Delta\omega$ Grid spacing in ω direction

ε Stretch function as given in Eq. (18)

η Total temperature recovery function as given in Eq. (4)

μ Absolute viscosity

ω Dimensionless radial coordinate equal to r/r_o

SUBSCRIPTS

e Conditions at probe entrance

i Local undisturbed conditions

s Conditions at shield surface

v Conditions at shield vent

w Conditions on the cone surface

∞ Conditions in the free stream

m Measured conditions